Voltammetry of Oxygen in the Room-Temperature Ionic Liquids 1-Ethyl-3-methylimidazolium Bis((trifluoromethyl)sulfonyl)imide and Hexyltriethylammonium Bis((trifluoromethyl)sulfonyl)imide: One-Electron Reduction To Form Superoxide. Steady-State and Transient Behavior in the Same Cyclic Voltammogram Resulting from Widely Different Diffusion Coefficients of Oxygen and Superoxide

Marisa C. Buzzeo,[†] Oleksiy V. Klymenko,[†] Jay D. Wadhawan,[†] Christopher Hardacre,[‡] Kenneth R. Seddon,[‡] and Richard G. Compton*[,†]

Physical and Theoretical Chemistry Laboratory, University of Oxford, South Parks Road, Oxford, OX1 3QZ, United Kingdom, and School of Chemistry, The Queen's University of Belfast, Belfast, Northern Ireland BT9 5AG, United Kingdom

Received: April 21, 2003; In Final Form: June 25, 2003

The electrochemical reduction of oxygen in two different room-temperature ionic liquids, 1-ethyl-3-methylimidazolium bis((trifluoromethyl)sulfonyl)imide ([EMIM][$N(Tf)_2$]) and hexyltriethylammonium bis((trifluoromethyl)sulfonyl)imide ([N_{6222}][$N(Tf)_2$]) was investigated by cyclic voltammetry at a gold microdisk electrode. Chronoamperometric measurements were made to determine the diffusion coefficient, *D*, and concentration, *c*, of the electroactive oxygen dissolved in the ionic liquid by fitting experimental transients to the Aoki model. [Aoki, K.; et al. *J. Electroanal. Chem.* **1981**, *122*, 19]. A theory and simulation designed for cyclic voltammetry at microdisk electrodes was then employed to determine the diffusion coefficient of the electrogenerated superoxide species, $O_2^{\bullet-}$, as well as compute theoretical voltammograms to confirm the values of *D* and *c* for neutral oxygen obtained from the transients. As expected, the diffusion coefficient of the superoxide species was found to be smaller than that of the oxygen in both ionic liquids. The diffusion coefficients of O_2 and $O_2^{\bullet-}$ in [N_{6222}][$N(Tf)_2$], however, differ by more than a factor of 30 ($D_{O_2} = 1.48 \times 10^{-10}$ m^2 s^{-1}, $D_{O_2^{\bullet-}} = 4.66 \times 10^{-12}$ m^2 s^{-1}), whereas they fall within the same order of magnitude in [EMIM][$N(Tf)_2$] ($D_{O_2} = 7.3 \times 10^{-10}$ m^2 s^{-1}, $D_{O_2^{\bullet-}} = 2.7 \times 10^{-10}$ m^2 s^{-1}). This difference in [N_{6222}][$N(Tf)_2$] causes pronounced asymmetry in the concentration distributions of oxygen and superoxide, resulting in significant differences in the heights of the forward and back peaks in the cyclic voltammograms for the reduction of oxygen. This observation is most likely a result of the higher viscosity of [N_{6222}][$N(Tf)_2$] in comparison to [EMIM][$N(Tf)_2$], due to the structural differences in cationic component.

Introduction

The electrochemical reduction of oxygen has been investigated extensively over the years in a wide variety of media.[1−10] As the generated superoxide, $O_2^{\bullet-}$, is a strong nucleophile and will readily disproportionate in water, the reduction of oxygen must be conducted in aprotic systems to produce stable superoxide ions. Dimethylformamide (DMF), acetonitrile (MeCN), and dimethyl sulfoxide (DMSO) are among the conventional nonaqueous solvents that have been employed for such investigation. In 1970, Merritt and Sawyer[11] studied the reactivity of electrochemically generated superoxide with alkyl halides in DMSO to give peroxide radicals via nucleophilic displacement of halide. The superoxide-initiated conversion of secondary nitroalkanes to ketones was investigated by Monte et al.[12] in 1983. Misra and Singh[13] reported the conversion of secondary alcohols to ketones by superoxide initiation, and Singh et al.[14] reported conversion of primary alcohols to carboxylic acids by similar methods.

More recently, room-temperature ionic liquids (RTILs) have been explored as solvents for the electrochemical detection of oxygen.[15−17] The characteristically negligible vapor pressure, high thermal stability, good conductivity, and wide potential window of RTILs makes them desirable solvents for the electrochemical investigation of a variety of electroactive species.[18] In 1991, Carter et al.[15] were among the first to study the one-electron reduction of oxygen

$$O_2 + e^- \rightarrow O_2^{-\bullet} \quad (1)$$

in room-temperature imidazolium chloride−aluminum chloride molten salts at a glassy-carbon disk electrode. The electrogenerated superoxide species, however, was unstable and no reverse current was observed in cyclic voltammetry at scan rates of 5−200 mV s^{-1} following the reduction of oxygen. The irreversibility was attributed to introduction of a proton source (H_2O) while the molten salt was saturated with O_2, despite efforts made to remove protons from the melt under vacuum. AlNashef et al.[16] reported the first evidence of the electrochemical generation of stable superoxide ions in the ionic liquid, 1-*n*-butyl-3-methylimidazolium hexafluorophosphate ([BMIM][PF_6]), proposing its potential role in low-temperature waste oxidation.

In this paper, we report the reduction of oxygen in [EMIM][$N(Tf)_2$] and [N_{6222}][$N(Tf)_2$] as detected by cyclic voltammetry

* To whom correspondence should be addressed. Tel: 01865 275413. Fax: 01865 275410. E-mail: Richard.Compton@chemistry.ox.ac.uk.
[†] University of Oxford.
[‡] The Queen's University of Belfast.

10.1021/jp0304834 CCC: $25.00
Published on Web 09/25/2003

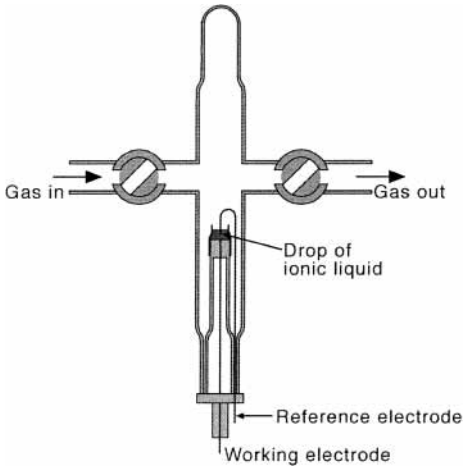

Figure 1. Cross-section of the cell used to conduct electrochemical experiments on 20 μL samples of [EMIM][N(Tf)$_2$] and [N_{6222}][N(Tf)$_2$].

(CV) at a gold microelectrode and the subsequent determination of the diffusion coefficients of oxygen and the electrogenerated superoxide species in the RTILs.

Experimental Section

Chemical Reagents. RTILs 1-ethyl-3-methylimidazolium bis((trifluoromethyl)sulfonyl)imide, [EMIM][N(Tf)$_2$] and hexyltriethylammonium bis((trifluoromethyl)sulfonyl)imide, [N_{6222}]-[N(Tf)$_2$] were synthesized from the corresponding bromide or chloride salts via a metathesis reaction in aqueous lithium bis-(trifluormethylsulfonyl)imide, as described by Bonhôte et al.[19] Ferrocene (Aldrich), tetrabutylammonium perchlorate (TBAP, Fluka) and acetonitrile (Fisher Scientific) were used directly without further purification. Impurity free oxygen, nitrogen, (BOC, Guildford, Surrey, U.K.) and carbon dioxide (Messer, Cedar House, Surrey, U.K.) were used for electrochemical experiments as described below.

Instrumentation. A commercially available potentiostat, PGSTAT 20 (Eco Chemie, Utrecht, The Netherlands), was used for the electrochemical experiments in conjunction with a Pentium-based PC. The 10 μm Au microdisk working electrode (Cypress Systems) comprised a Au wire sealed in borosilicate glass which was carefully polished using a 1.0 μm alumina slurry (Kermet, Kent, U.K.), followed by a 0.3 μm alumina suspension (Buehler, Lake Bluff, IL). The electrode was then polished on a clean, damp cloth (Microcloth, Buehler, Lake Bluff, IL), immersed in 10% nitric acid solution to remove any adsorbates, and then rinsed with acetonitrile. The diameter of the microdisk electrode was calibrated electrochemically using 2 mM ferrocene in 0.1 M TBAP/acetonitrile, using a value for the diffusion coefficient of 2.3×10^{-5} cm^2 s^{-1} at 20 °C.[20]

For all electrochemical experiments, a short piece (~2 cm long) of heat-shrink tubing was fit around the glass surrounding the working electrode to provide a casing, to which ~20 μL of ionic liquid was delivered by micropipet. For those electrochemical experiments performed in [EMIM][N(Tf)$_2$], the outer circumference of the glass was coated with silver-loaded conducting paint (RS Chemicals), which acted as a counter/reference electrode. For those conducted in [N_{6222}][N(Tf)$_2$], a silver wire was secured around the heat-shrink tubing, acting as a counter/reference electrode. All experiments were carried out in an electrochemical cell designed to sustain a vacuum conditions at a temperature of 20 ± 3 °C (see Figure 1).

Prior to the addition of gases, the sample of ionic liquid was placed under vacuum (Edwards High Vacuum Pump, Model ES 50) for 90 min or until the baseline showed little trace of atmospheric oxygen. Oxygen was introduced to the electrochemical cell in increasing ratios using a Wösthoff triple gas-mixing pump (Bochum, Germany), accurate to ±1%. Nitrogen made up the remainder of the gas mixture. Gas mixtures were passed through the cell for at least 30 min before final measurements were taken to ensure that equilibration of the gases and the ionic liquid had been established.

Theory

Transients. To determine the concentration and the diffusion coefficient of oxygen in the ionic liquids, chronoamperometric experiments were performed at the Au microdisk electrode. Theoretical transients were then calculated according to the Aoki model,[21] whereby the current−time curve following a potential step at a microdisk electrode is given by

$$i = 4nFr_eD_oc_o\, f(\tau) \tag{2}$$

where n is the number of electrons transferred, F is the Faraday constant (96 485 C mol^{-1}), r_e is the radius of the microdisk, D_o is the diffusion coefficient of the electroactive species, c_o is the concentration of the electroactive species, and the dimensionless parameter, τ, is defined as $\tau = 4Dt/r_e^2$. The function $f(\tau)$ depends on the value of τ, which is an index of time, t. At longer times, when $\tau > 0.82$

$$f(\tau) = 1 + 0.71835\tau^{-1/2} + 0.0562\tau^{-3/2} - 0.0064\tau^{-5/2} \tag{3}$$

Equation 3 was used to generate theoretical transients using a nonlinear curve fitting program available in Origin 6.0 (Microcal Software, Inc.). Having specified the radius of the microdisk, the computer software optimized the fit between the experimental and theoretical transients by varying the values of the diffusion coefficient and concentration of the electroactive species, O_2. The accuracy of these values was then verified and a value for the diffusion coefficient of the superoxide was determined using a computer program designed to simulate cyclic voltammograms at microelectrodes as described in the following section.

Simulation of Cyclic Voltammograms

The time dependent equations describing the mass transport of the species to a microdisk electrode of radius r_e written in the cylindrical coordinates r, z are

$$\frac{\partial[\mathrm{A}]}{\partial t} = D_\mathrm{A}\left(\frac{\partial^2[\mathrm{A}]}{\partial r^2} + \frac{1}{r}\frac{\partial[\mathrm{A}]}{\partial r} + \frac{\partial^2[\mathrm{A}]}{\partial z^2}\right)$$
$$\frac{\partial[\mathrm{B}]}{\partial t} = D_\mathrm{B}\left(\frac{\partial^2[\mathrm{B}]}{\partial r^2} + \frac{1}{r}\frac{\partial[\mathrm{B}]}{\partial r} + \frac{\partial^2[\mathrm{B}]}{\partial z^2}\right) \tag{4}$$

where D_A and D_B are the diffusion coefficients of oxygen and superoxide. The solution is assumed to contain the O_2 species only at the beginning of the electrolysis. It follows that the initial conditions for the partial differential equations (4) are

$$[\mathrm{A}] = c_0 \qquad [\mathrm{B}] = 0 \tag{5}$$

The boundary conditions corresponding to the cyclic voltammetric conditions are as follows:

$$
\begin{aligned}
z = 0,\ 0 \le r \le r_e \qquad & D_A \left.\frac{\partial[A]}{\partial z}\right|_{z=0} = (k_f[A] - k_b[B])_{z=0}; \\
& D_B \left.\frac{\partial[B]}{\partial z}\right|_{z=0} = -D_A \left.\frac{\partial[A]}{\partial z}\right|_{z=0} \\
z = 0,\ r > r_e \qquad & \left.\frac{\partial[A]}{\partial z}\right|_{z=0} = \left.\frac{\partial[B]}{\partial z}\right|_{z=0} = 0 \\
\text{all } z,\ r = 0 \qquad & \left.\frac{\partial[A]}{\partial r}\right|_{r=0} = \left.\frac{\partial[B]}{\partial r}\right|_{r=0} = 0 \\
z,\ r \to \infty \qquad & [A] \to [A]_{bulk}; \qquad [B] \to 0
\end{aligned} \tag{6}
$$

where k_f and k_b (cm s^{-1}) denote the forward and reverse rates for the reduction of O_2, which have a potential dependence described by the Butler−Volmer theory as

$$
\begin{aligned}
k_f &= k_0 \exp\left(\frac{-\alpha F}{RT}(E - E_f^\circ)\right) = k_0 \exp(-\alpha\theta) \\
k_b &= k_0 \exp\left(\frac{(1-\alpha) F}{RT}(E - E_f^\circ)\right) = k_0 \exp((1-\alpha)\theta)
\end{aligned} \tag{7}
$$

where α is the transfer coefficient, E_f° is the formal electrode potential, $\theta = (F/(RT))(E - E_f^\circ)$ is the dimensionless potential, k_0 is the standard electrochemical rate constant, R is the universal gas constant, and T is the absolute temperature.

The initial half-infinite simulation area in the cylindrical coordinates r, z was mapped onto a closed box using the coordinate transformation developed by Amatore and Fosset.[22] The application of this transformation allows one to handle the edge singularity that arises from the nonuniform accessibility of the microdisk electrode that is reflected in the discontinuous boundary conditions (6). The transformation is given by the following equations

$$
R = \frac{\sqrt{1-\theta^2}}{\cos\left(\frac{\pi}{2}\Gamma\right)}; \qquad Z = \theta \tan\left(\frac{\pi}{2}\Gamma\right) \tag{8}
$$

where $R = r/r_e$ and $Z = z/r_e$. The normalized R, Z space and the transformed θ, Γ space are shown in Figure 2.

The alternating direction implicit (ADI) method[23−25] was used to solve the mathematical model (4)−(6), rewritten in the transformed coordinates, numerically in two dimensions. The ADI method applied to the problem under consideration produces banded pentadiagonal systems of linear equations, which allowed the use of the generalized Thomas algorithm[25] for their solution.

The current flowing at the electrode surface was calculated using the expression

$$
i = -2\pi F D_A \int_0^{r_d} \left(\frac{\partial[A]}{\partial z}\right)_{z=0} r\, dr \tag{9}
$$

The computer program implementing the ADI method for the mathematical model (4)−(6) was written in Borland Delphi 6 Professional Edition and executed on a PC with Intel Pentium 4 2GHz and 1 Gb of RAM.

The numerical convergence of the described simulation procedure has been examined elsewhere[26] for the case of conventional solvents such as water or acetonitrile. The species taking part in a simple E-reaction in such a solvent usually have virtually equal diffusion coefficients.[27] It has been shown earlier that in this case the spatial grid size necessary for simulation

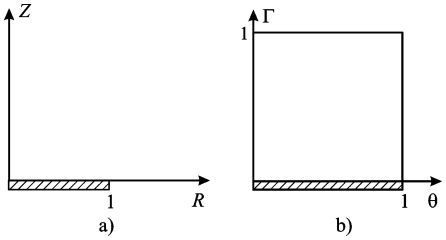

Figure 2. Normalized physical space (R, Z) and the simulation space (θ,Γ) after the coordinate transformation (8).

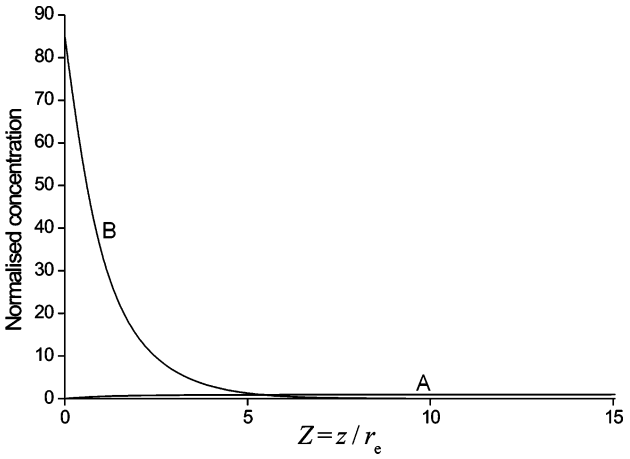

Figure 3. Concentration distribution of species taking part in the oxidation reaction corresponding to the top of the steady-state voltammogram for the case when $D_A = 100D_B$. The normalized concentration is plotted vs the normalized distance from the electrode and corresponds to the distribution along the normal to the electrode surface at its center.

of voltammetry within 0.1% error is 60 × 60 ($N\theta \times N\Gamma$).[26] However, in the case of ionic electrolyte the diffusion coefficients of initial and reduced/oxidized species may differ significantly (which will be shown below to be the case for the oxygen reduction in $[N_{6222}][N(Tf)_2]$). The difference between the diffusion coefficients causes asymmetrical concentration distribution of the initial neutral species and reduced/oxidized species. Figure 3 shows the concentration distribution of species A and B along the normal to the electrode surface at its center corresponding to the top of the quasi-steady-state voltammogram for the case when the diffusion coefficients are different by a factor of 100 ($D_A = 100D_B$). It can be seen from the figure that there is a huge build-up of the concentration of B near the electrode surface due to low diffusivity of the latter. The concentration gradient of species B is much higher than that of A. At the same time the diffusion layer thickness for A, which is conventionally expressed for a pure diffusion process as $6\sqrt{D_A t^*}$ where t^* is the electrolysis duration, is about 10 times larger than the diffusion layer thickness for B. This fact creates difficulties for the numerical methods because the concentration profiles of different species are represented with different levels of accuracy due to the enormous difference in the concentration gradients and discrete nature of the solution. The conditions become even worse for high voltage scan rates when the diffusion layer thicknesses become smaller. Therefore, to obtain better discretization of the steep concentration profile of species B, the simulation grid has to be much finer than for the case of equal diffusion coefficients to attain the same level of accuracy.

For the reasons described above, the simulation method was tested to find the grid sizes that give reasonable values of convergence. Figure 4 shows the dependence of the convergence error in the forward and reverse peak currents on the number

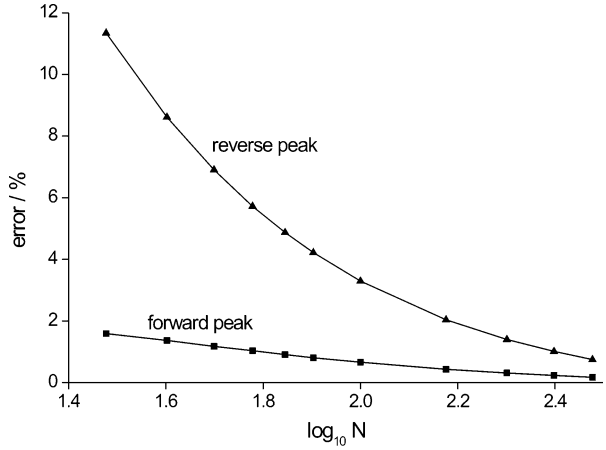

Figure 4. Convergence error for the forward and reverse peaks against the number of grid points $N = N\theta = N\Gamma$ simulated for $D_A/D_B = 100$ and scan rate of 1 V s^{-1}.

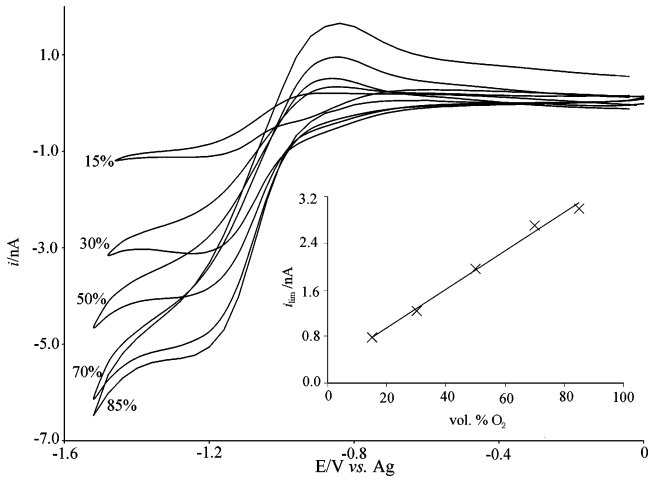

Figure 5. Cyclic voltammograms (1 V s^{-1} scan rate) for the reduction of O_2 in [EMIM][$N(Tf)_2$] at a 10.8 μm Au microdisk electrode at varying volume % O_2. The inset shows a plot of limiting current vs volume % O_2. The error bar for the values of the limiting current is $\pm$0.29 nA.

of grid points in both θ and Γ directions ($N = N\theta = N\Gamma$). The values of the convergence error were obtained by simulating a cyclic voltammogram with increasing grid size and comparing the resulting peak currents to their "converged" values simulated at a grid of the size 700 $\times$ 700 ($N\theta \times N\Gamma$). In all cases the number of time steps was chosen to be 5000. All simulations for Figure 4 were performed for the scan rate of 1 V s^{-1}, which was the fastest used in the experiment and for the diffusion coefficients satisfying the ratio $D_A/D_B = 100$ which was higher than the expected ratio of the diffusion coefficients of O_2 and $O_2^{\bullet-}$ (see below). Thus the convergence data in Figure 4 have some "safety margin" for further analysis.

Results and Discussion

Figure 5 shows the cyclic voltammograms for the one-electron reduction of oxygen at a 10.8 μm Au microdisk electrode in [EMIM][$N(Tf)_2$] in increasing volume percent from 15% to 85%, with nitrogen making up the remainder of the gas mixture. The half-wave potential occurs at -0.98 V vs Ag, which is similar to that previously reported.[16] in [BMIM][PF_6]. It can be seen from the inset in Figure 5 that the current observed for the one-electron reduction is directly proportional to the percent volume of O_2. Additionally, the presence of the back peak,

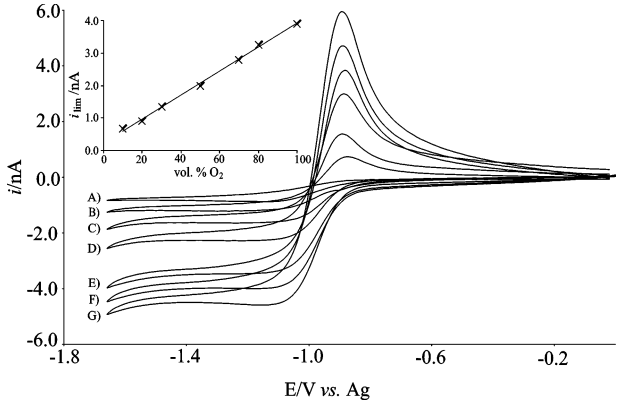

Figure 6. Cyclic voltammograms (1 V s^{-1} scan rate) for the reduction of O_2 in [N_{6222}][$N(Tf)_2$] at a 10.8 μm Au microdisk electrode at varying volume % O_2: (A) 10, (B) 20, (C) 30, (D) 50, (E) 70, (F) 80, and (G) 90 vol % O_2. The inset shows a plot of limiting current vs volume % O_2. The error bar for the values of the limiting current is $\pm$0.23 nA.

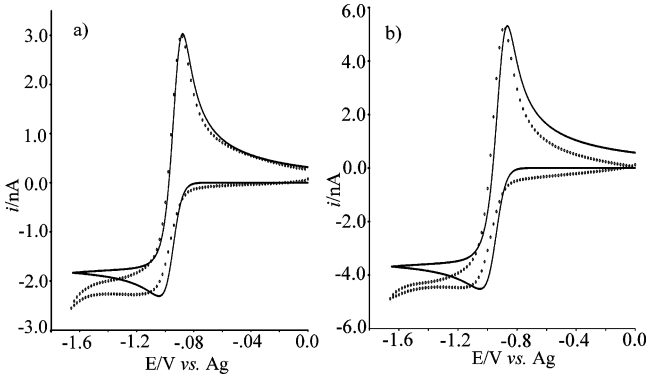

Figure 7. Comparison of experimental and simulated voltammograms (1 V s^{-1} scan rate) for the reduction of oxygen in [N_{6222}][$N(Tf)_2$] in (a) 50% O_2 50% N_2 and (b) 90% O_2 10% N_2 gas mixtures. The open circles represent experimental data and the solid line represents simulated data.

which corresponds to the oxidation of superoxide back to oxygen, gives evidence that the generated superoxide is stable and the reduction of oxygen is electrochemically reversible in this system. The asymmetry of the forward and reverse peaks is similar to that observed by AlNashef[16] in [BMIM][PF_6] and reflects the difference in the diffusion type of oxygen versus superoxide: under the conditions examined, the diffusion of oxygen to the electrode is almost spherical (steady state) whereas the diffusion of superoxide is virtually planar.

Figure 6 shows the cyclic voltammograms for the electrochemically reversible reduction of oxygen over the range 10$-$100 volume percent at a 10.8 μm Au microdisk electrode in [N_{6222}][$N(Tf)_2$], with a half-wave potential at -0.85 V vs Ag. The positive shift of the reduction potential in [N_{6222}][$N(Tf)_2$] compared to [BMIM][PF_6] is consistent with previous evidence that the potential shifts to more positive values as the solvating properties of the solvent increase.[16] Again, the plot of current versus percent volume of O_2 (Figure 6, inset) shows good linearity for the signal observed for the one-electron reduction. As can be seen from the difference in heights of the forward and back peaks, there is an even greater discrepancy in diffusion coefficients between the neutral and charged species in this ionic liquid. Although the charged $O_2^{\bullet-}$ species is expected to travel more slowly through the ionic liquid, the exaggerated difference in the rates of diffusion was of particular note. This observation is attributed to the increased viscosity of the tetraalkylammonium salt compared to the imidazolium salt.

Though [EMIM][$N(Tf)_2$] and [N_{6222}][$N(Tf)_2$] share the same bis((trifluoromethyl)sulfonyl)imide anion, the structural differ-

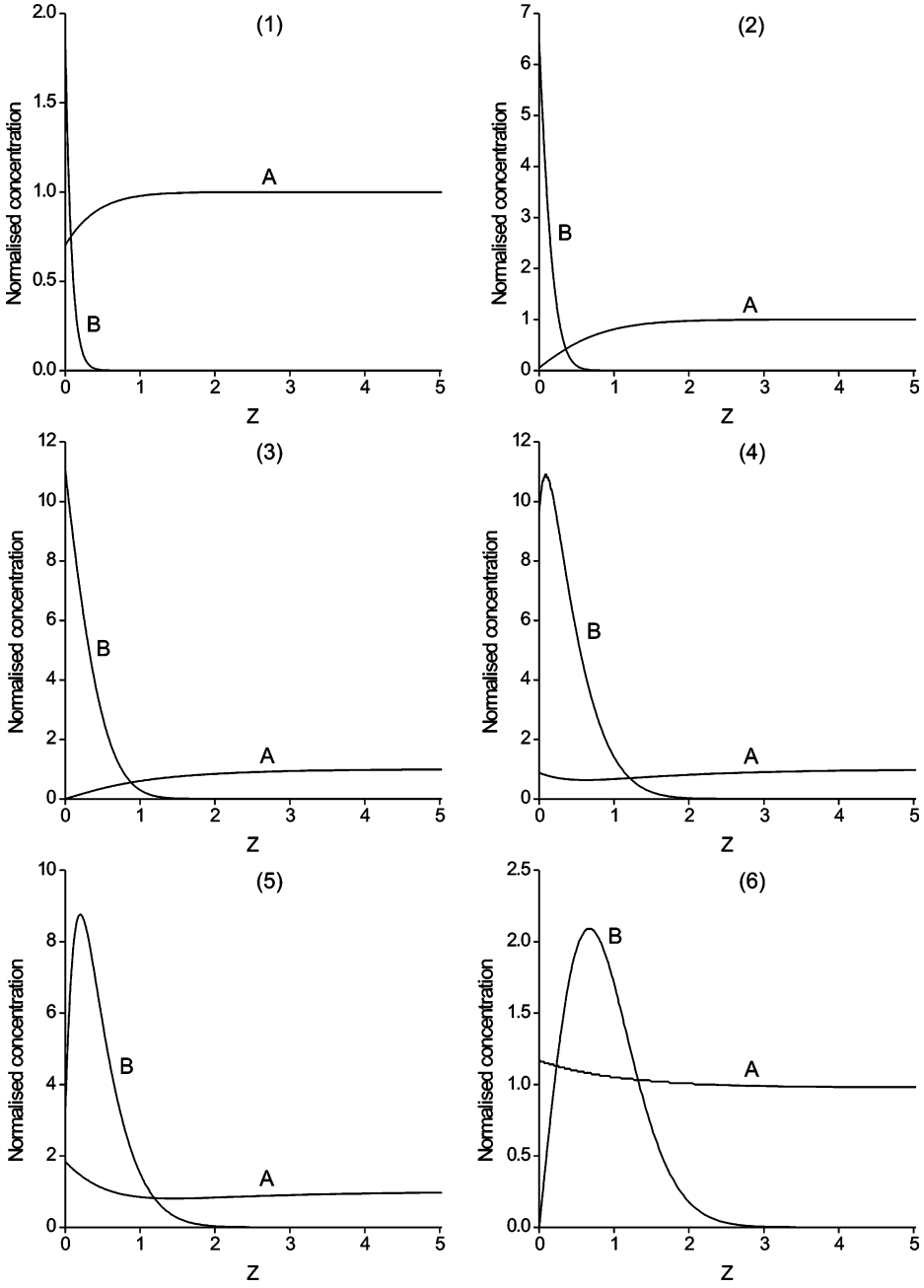

Figure 8. Concentration distributions of oxygen (A) and superoxide (B) simulated for several specific points at the voltammogram (see Figure 9). Normalized concentration distributions along the central normal to the electrode surface are plotted against the normalized distance $Z = (z/r_e)$.

ences in their cationic component has significant implications. The tetraalkylammonium cation is more electrochemically stable than the imidazolium cation, resulting in a much wider potential window for $[N_{6222}][N(Tf)_2]$.[28] Additionally, increasing the alkyl chain length and/or fluorination of the cationic component has been shown to increase the ionic liquid's viscosity due to increased van der Waals interactions.[19] Measurements by Hardacre et al.[29,30] reported a value of 32.1 cP for the viscosity of $[EMIM][N(Tf)_2]$, compared to 220 cP for $[N_{6222}][N(Tf)_2]$.

To determine the concentration and diffusion coefficient of oxygen in the two ionic liquids, chronoamperometric measurements were taken at the gold microdisk electrode. The samples were placed under vacuum for at least 90 min and then equilibrated with 100 vol % oxygen. The potential applied to the working electrode was held for 300 s initially and then stepped from 0.0 V vs Ag, corresponding to no Faradaic current, to −1.45 V vs Ag, a potential well past the E_f° value for the one-electron reduction of oxygen. These experimental transients were then fitted using a nonlinear curve fitting program according to the Aoki model,[21] which provides an equation for the time-dependent current curve generated at microdisk electrodes, as described in a previous section. This program was able to determine best-fit values of D_{O_2} and c_{O_2} by optimizing the parameters so that there was minimal discrepancy between the theoretical and experimental transients. The concentration of oxygen in a saturated sample of $[EMIM][N(Tf)_2]$ was found to be 3.9 mM, which is in close agreement with the value of 3.6 mM previously reported for O_2 in $[BMIM][PF_6]$.[16,31] In $[N_{6222}][N(Tf)_2]$, however, the concentration of oxygen was found to be 11.6 mM, more than 3 times greater than in $[EMIM][N(Tf)_2]$. With the obtained concentration values, the Henry's Law constant, K_H, can be calculated by rearrangement of the following equation:

$$c_A = K_H P_A \tag{10}$$

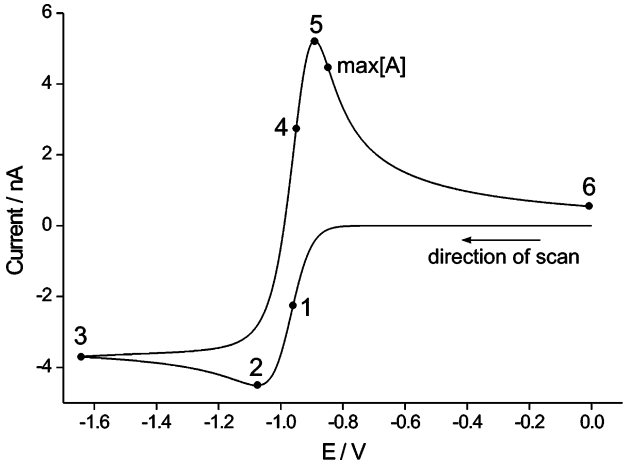

Figure 9. Simulated cyclic voltammogram for the scan rate of 1 V s^{-1} with the specific points marked. The concentration distributions corresponding to the points are shown in Figure 8. The point marked as "max [A]" corresponds to the maximum surface concentration of oxygen.

where c_A is concentration of A and P_A is the partial pressure of A. $K_H = 3.9$ mM atm^{-1} for [EMIM][$N(Tf)_2$] and $K_H = 11.6$ mM atm^{-1} for [N_{6222}][$N(Tf)_2$]. The diffusion coefficient value for O_2 in [EMIM][$N(Tf)_2$], as determined from the transient fitting, was $D_{O_2} = 8.3 \times 10^{-10}$ m^2 s^{-1}, and the value found in [N_{6222}][$N(Tf)_2$] was $D_{O_2} = 1.5 \times 10^{-10}$ m^2 s^{-1}. As expected, the diffusion of oxygen in the more viscous ionic liquid was much slower, by approximately a factor of 6. These obtained parameters were then used in conjunction with the previously determined electrode radius to simulate cyclic voltammograms to verify their accuracy and to obtain a value of the diffusion coefficient of the generated superoxide.

Determination of the diffusion coefficient of the superoxide species, $O_2^{\bullet-}$ in [N_{6222}][$N(Tf)_2$] was of particular interest given its significant variation from D_{O_2}. Using the value of D_{O_2} obtained from fitting of the transients as an initial approximation, the values of D_{O_2} and $D_{O_2^{\bullet-}}$ were adjusted to optimize the fit between experimental and simulated voltammograms, holding c_{O_2}, and r_e constant. As previously stated, though the diffusion coefficient of the electrogenerated superoxide is smaller than that of the oxygen for both RTILs, there is a pronounced difference observed in the more viscous [N_{6222}][$N(Tf)_2$] ionic liquid. The average value of D_{O_2} in [EMIM][$N(Tf)_2$] was 7.3×10^{-10} m^2 s^{-1}, which is in fair agreement with a value of 2.2×10^{-10} m^2 s^{-1} reported for oxygen in [BMIM][PF_6].[16] The average value of $D_{O_2^{\bullet-}}$ in [EMIM][$N(Tf)_2$] was 2.7×10^{-10} m^2 s^{-1}. In [N_{6222}][$N(Tf)_2$], however, the average value of D_{O_2} was 1.48×10^{-10} m^2 s^{-1} whereas the average value of $D_{O_2^{\bullet-}}$ was 4.66×10^{-12} m^2 s^{-1}, differing by more than 1 order of magnitude. All simulations were run with the grid size of $300 \times 300 \times 3000$ ($N\theta \times N\Gamma \times Nt$) to ensure that the convergence error was less than 1%. A typical simulation time for these parameters was around 4.5 min. Selected examples of simulated voltammograms for the reduction of oxygen at 1 V s^{-1} are shown with comparison to the experimental CVs for [N_{6222}][$N(Tf)_2$] in Figure 7.

Last, we consider the concentration distributions (Figure 8) of oxygen (A) and superoxide (B) along the normal to the electrode surface at the disk center for different specific points at the cyclic voltammogram represented in Figure 9. The concentrations are normalized as $[A]/c_0$ and $[B]/c_0$ and plotted against the normalized distance from the electrode surface $Z = z/r_e$. The concentration profiles 1−3 in Figure 8 exhibit the same behavior as has been shown in the previous section. The thickness of the diffusion layer of oxygen is much bigger than that of the superoxide due to the difference in the diffusion coefficients by a factor of around 30. Thus, a large amount of superoxide is concentrated in the vicinity of the electrode surface, providing the diffusion layer thickness of a small fraction of the electrode radius, which is typical for transient microdisk behavior. This gives rise to high currents on the reverse scan (Figure 8, profiles 4−6). This also gives rise to the concentration of oxygen at the electrode surface as the large amount of superoxide gets oxidized during the reverse scan (Figure 8, profiles 4−6). The maximum value of the concentration of oxygen at the electrode surface for the voltammogram considered is 2 times larger than the bulk concentration and is reached at a potential $E = -0.8525$ V at the reverse scan.

Conclusions

The one-electron reduction of oxygen has been investigated by cyclic voltammetry at a gold microdisk electrode in the RTILs, 1-ethyl-3-methylimidazolium bis((trifluoromethyl)sulfonyl)imide ([EMIM][$N(Tf)_2$]) and hexyltriethylammonium bis((trifluoromethyl)sulfonyl)imide ([N_{6222}][$N(Tf)_2$]). The combination of chronoamperometric measurements and a simulation program designed for cyclic voltammetry at a microdisk electrode allowed for the determination of the diffusion coefficient, D, and concentration, c, of the neutral oxygen, as well as the diffusion coefficient of the electrogenerated superoxide. The higher viscosity of [N_{6222}][$N(Tf)_2$] compared to [EMIM][$N(Tf)_2$]), due to structural variation in the cationic components, resulted in significantly different diffusion coefficients of oxygen and superoxide, differing by more than a factor of 30.

Acknowledgment. M.C.B. thanks the Analytical Division of The Royal Society of Chemistry for a studentship and Alphasense for CASE funding. O.V.K. thanks the Clarendon fund for partial support. J.D.W. thanks the EPSRC for a studentship.

References and Notes

(1) Hahn, C. E. W. *Clin. Phys. Physiol. Meas.* **1987**, *8*, 3.
(2) Hahn, C. E. W. *Analyst* **1988**, *123*, 57R.
(3) Clark, L. C. *Trans. Am. Soc. Artif. Intern. Organs* **1956**, *2*, 41.
(4) Albery, W. J.; Barron, P. *J. Electroanal. Chem.* **1982**, *79*.
(5) Hahn, C. E. W.; McPeak, H.; Bond, A. M.; Clark, D. *J. Electroanal. Chem.* **1995**, *393*, 61.
(6) Roberts, J. L., Jr.; Sawyer, D. T. *J. Electroanal. Chem.* **1966**, 90.
(7) Lund, W.; Peover, M. E. *J. Electroanal. Chem.* **1970**, *25*, 19.
(8) Fujinaga, T.; Izutsu, K.; Adachi, T. *Bull. Chem. Soc. Jpn.* **1969**, *42*, 140.
(9) Wadhawan, J. D.; Welford, P. J.; Maisonhaute, E.; Climent, V.; Lawrence, N. S.; Compton, R. G.; McPeak, H.; Hahn, C. E. W. *J. Phys. Chem. B* **2001**, *105*, 10659.
(10) Wadhawan, J. D.; Welford, P. J.; McPeak, H. B.; Hahn, C. E. W.; Compton, R. G. *Sens. Actuators B* **2003**, *88*, 40.
(11) Merritt, M. V.; Sawyer, D. T. *J. Org. Chem.* **1970**, *35*, 2157.
(12) Monte, W. T.; Baizer, M. M.; Little, R. D. *J. Org. Chem.* **1983**, *48*, 803.
(13) Singh, M.; Misra, R. A. *Synthesis* **1989**, 403.
(14) Singh, M.; Krishna, N.; Singh, S. D.; Misra, R. A. *Synthesis* **1991**, 291.
(15) Carter, M. T.; Hussey, C. L.; Strubinger, S. K. D.; Osteryoung, R. A. *Inorg. Chem.* **1991**, *30*, 1149.
(16) AlNashef, I. M.; Leonard, M. L.; Kittle, M. C.; Matthews, M. A.; Weidner, J. W. *Electrochem. Solid-State Lett.* **2001**, *4*, D16.
(17) AlNashef, I. M.; Leonard, M. L.; Matthews, M. A.; Weidner, J. W. *Ind. Eng. Chem. Res* **2002**, *41*, 4475.
(18) Welton, T. *Chem. Rev.* **1999**, *99*, 2071.
(19) Bonhôte, P.; Dias, A.-P.; Papageorgiou, N.; Kalyanasundaram, K.; Grätzel, M. *Inorg. Chem.* **1996**, *35*, 1168.
(20) Sharp, P. *Electrochim. Acta* **1983**, *28*, 301.

(21) Aoki, K.; Osteryoung, J. *J. Electroanal. Chem.* **1981**, *122*, 19.
(22) Amatore, C.; Fosset, B. *J. Electroanal. Chem.* **1992**, *328*, 21.
(23) Heinze, J. *Electroanalysis* **1981**, *124*, 73.
(24) Heinze, J.; Storzbach, M. *Ber. Bunsen-Ges. Phys. Chem.* **1986**, *90*, 1043.
(25) Svir, I. B.; Klymenko, O. V.; Compton, R. G. *Radiotekhnika* **2001**, *118*, 92.
(26) Rees, N. V.; Klymenko, O. V.; Compton, R. G.; Oyama, M. *J. Electroanal. Chem.* **2002**, *531*, 33.
(27) Wang, R. L.; Tam, K. Y.; Compton, R. G. *J. Electroanal. Chem.* **1997**, *434*, 105.
(28) Sun, J.; Forsyth, M.; MacFarlane, D. R. *J. Phys. Chem. B* **1998**, *102*, 8858.
(29) Evans, R. G.; Klymenko, O. V.; Hardacre, C.; Seddon, K. R.; Compton, R. G. *J. Electroanal. Chem.*, in press.
(30) Hardacre, C.; Holbrey, J. D.; Katdare, S. P.; Seddon, K. R. *Green Chemistry* **2002**, *4*, 143.
(31) Anthony, J. L.; Maginn, E. J.; Brennecke, J. F. *J. Phys. Chem. B* **2002**, *106*, 7315.